



Published in final edited form as:

*Clin Nucl Med.* 2012 September ; 37(9): 854–861. doi:10.1097/RLU.0b013e318262c76a.

## Comparison of F-18 Fluorodeoxyglucose and F-18 Fluorothymidine Positron Emission Tomography in Differentiating Radiation Necrosis from Recurrent Glioma

Michael S. Enslow<sup>2</sup>, Lauren V. Zollinger<sup>1</sup>, Kathryn A. Morton<sup>1,3</sup>, Dan J. Kadrmaz<sup>1,3</sup>, Regan I. Butterfield<sup>3</sup>, Paul E. Christian<sup>3</sup>, Kenneth M. Boucher<sup>3,4</sup>, Marta E. Heilbrun<sup>1</sup>, Randy L. Jensen<sup>3</sup>, and John M. Hoffman<sup>1,3</sup>

<sup>1</sup>Radiology, University of Utah, Salt Lake City, UT

<sup>2</sup>School of Medicine, University of Utah, Salt Lake City, UT

<sup>3</sup>Huntsman Cancer Institute, University of Utah, Salt Lake City, UT

<sup>4</sup>Oncologic Sciences, University of Utah, Salt Lake City, UT

### Abstract

**Purpose of the Report**—The objective was to compare F-18 fluorodeoxyglucose (FDG) and F-18 fluorothymidine (FLT) positron emission tomography (PET) in differentiating radiation necrosis from recurrent glioma.

**Materials and methods**—Visual and quantitative analyses were derived from static FDG PET and static and dynamic FLT PET in 15 patients with suspected recurrence of treated grade II glioma with a new focus of Gd-contrast enhancement on MRI. For FDG PET, SUV<sub>max</sub> and the ratio of lesion SUV<sub>max</sub> to the SUV<sub>mean</sub> of contralateral white matter were measured. For FLT PET, SUV<sub>max</sub> and Patlak-derived metabolic flux parameter Ki<sub>max</sub> were measured for the same locus. A 5-point visual confidence scale was applied to FDG PET and FLT PET. ROC analysis was applied to visual and quantitative results. Differences between recurrent tumor and radiation necrosis were tested by Kruskal-Wallis analysis. Based on follow-up Gd-MRI imaging, lesion-specific recurrent tumor was defined as a definitive increase in size of the lesion, and radiation necrosis as stability or regression.

**Results**—For FDG SUV<sub>max</sub>, FDG ratio lesion:white matter and FLT Ki<sub>max</sub>, there was a significant difference between mean values for recurrent tumor and radiation necrosis. Recurrent tumor was best identified by FDG ratio of lesion:contralateral normal white matter (AUC 0.98, CI 0.91–1.00, sens. 100%, spec. 75% for an optimized cut-off value of 1.82).

**Conclusion**—Both quantitative and visual determinations allow accurate differentiation between recurrent glioma and radiation necrosis by both FDG and FLT PET. In this small series, FLT PET offers no advantage over FDG PET.

### Keywords

Fluorothymidine; FLT; fluorodeoxyglucose; FDG; positron emission tomography; PET; brain; tumor; glioma; radiation necrosis; recurrence; magnetic resonance imaging; MRI; gadolinium; Gd

## INTRODUCTION

There are approximately 16,900 new cases of primary CNS tumors diagnosed in the United States each year. The incidence of these tumors has increased significantly in the last decades (1). About 50% of these lesions are supratentorial high-grade gliomas. Anaplastic astrocytoma (WHO Grade III) and glioblastoma multiforme (GBM) (WHO grade IV) are the most common glial primary brain tumors (2, 3). Patients with newly diagnosed malignant gliomas are usually treated with surgical debulking or resection, followed by radiation therapy and/or chemotherapy, depending on their functional status. With recent advances in chemotherapy, such as temozolomide and combined modality treatment for glial brain tumors, the proportion of long-term survivors has increased from less than 5% to between 15–20 % (4). However, overall survival for GBM remains poor even with the addition of temozolomide drug therapy. A recent study showed a median survival of 14.6 months with radiotherapy plus temozolomide and 12.1 months with radiotherapy alone (5).

A particularly problematic aspect of the management of patients with brain tumors is the development of a new enhancing lesion on a gadolinium enhanced magnetic resonance imaging (Gd-MRI) within the radiation field which could indicate either recurrent tumor or radiation necrosis. The distinction between these two entities is difficult by conventional imaging techniques alone and typically requires either biopsy or longitudinal observation which complicates and greatly affects short term patient management.

F-18 fluorodeoxyglucose (FDG) positron emission tomography (PET) has been used to differentiate recurrent tumor from radiation necrosis for nearly 30 years (6). The literature reveals disparity in the performance of F-18 FDG PET for this application. Typical sensitivities are reported between 81 – 86%, although some results are reported to be greater, up to 100% (7–11). Sensitivity may be complicated by high metabolic activity in adjacent cortex and partial volume effects due to small lesions. Estimates of specificity are lower, ranging from 22 to 92%. Specificity may be compromised by metabolic activity in areas of post-treatment inflammatory change.

F-18 fluoro-labeled thymidine (FLT) is a radiopharmaceutical that has been shown to directly assess tumor proliferation using PET (12–16). F-18 FLT PET has been shown to be a marker of tumor aggressiveness and overall therapeutic response (14–17). F-18 FLT does not localize to normal brain due to low proliferative activity and because it does not cross an intact blood-brain barrier. Methods have been developed and validated to model the kinetic features of F-18 FLT PET by tumors, and the necessity for this kinetic modeling is thought to be critical in distinguishing non-specific uptake of FLT from that pertaining to new DNA synthesis and cell proliferation (15, 18–20). Several studies have shown significant F-18 FLT uptake in higher-grade primary brain tumors (21–23). To date, only one preliminary published comparison has been made between F-18 FLT PET and F-18 FDG PET in distinguishing recurrent glioma from radiation necrosis, and this report showed a significantly poorer performance of F-18 FDG PET than typically reported elsewhere (24). The primary objective of the current study is to compare the efficacy of quantitative and visual assessments of F-18 FDG and F-18 FLT PET in differentiating radiation necrosis from recurrent moderate to high grade ( grade II) gliomas.

## MATERIALS AND METHODS

### Patient Eligibility

All studies were performed with IRB approval and the provision of signed informed consent by each patient. Enrolled subjects included 15 evaluable adult patients (9 males, 6 females; ages 22–75) with histologically proven grade II glial-based primary brain tumors. All

patients had been treated with radiation, with or without chemotherapy. Radiation therapy had been completed a minimum of 4 months prior to study entry. All subjects had a new enhancing lesion within the radiation field demonstrated by a clinical Gd-MRI. This lesion was interpreted as consistent with either radiation necrosis or recurrent tumor. All subjects had also undergone a clinical F-18 FDG PET of the brain within one month of the Gd-MRI for the purpose of differentiating radiation necrosis from tumor recurrence. Enrolled subjects consented to undergo an additional PET scan with F-18 FLT, which in all cases was performed within 3 weeks of the clinical F-18 FDG PET.

Exclusion criteria included: Pregnancy or lactation (a negative pregnancy test was required for premenopausal females); clinically significant signs of uncal herniation (such as acute pupillary enlargement, rapidly developing motor changes or rapidly decreasing level of consciousness); known allergic or hypersensitivity reactions to previously administered radiopharmaceuticals; and the requirement of monitored anesthesia for PET scanning.

### Gd-MRI

All Gd-MRI scans were performed according to clinical protocols on Siemens 1.5T or 3T systems (Erlangen, Germany) with the following parameters: sagittal T1 fast spin echo (FSE), axial T1 FSE, axial T2 FSE, axial FLAIR inversion-recovery, axial gradient-recalled-echo (GRE), axial diffusion tensor imaging (DTI) or diffusion-weighted imaging (DWI), as well as axial and coronal T1 weighted images following the administration of intravenous gadolinium (Gd-DTPA). The presence of a new or enlarging area of enhancement within the radiation port, and follow-up assessment of progression, stability or regression of this specific lesion was characterized by an experienced neuroradiologist (LZ), independent of a separate clinical report.

### F-18 FDG PET

All F-18 FDG PET scans were performed according to clinical protocol. Patient preparation included 6 hours without caloric intake or insulin administration. 370 MBq (10 mCi) of F-18 FDG was given intravenously through a peripheral vein. Patients rested quietly in a recliner during the uptake interval (45 minutes), without physical activity and with minimal vocalization. A F-18 FDG PET scan was performed for 30 min over a single bed position using a GE Advance PET scanner (Milwaukee, WI) in 3-D mode, with transmission attenuation correction performed for 5 minutes using a rotating  $^{68}\text{Ge}$  rod source. Images were reconstructed using the 3D reprojection algorithm.

### F-18 FLT PET

The F-18 FLT studies were investigational and conducted under an investigational new drug (IND) for FLT. The  $^{18}\text{F}$ -FLT was synthesized by methods previously reported (25, 26), FLT average specific activity was 7368 Ci/mmol (5,170–11,669 Ci/mmol). Following positioning for a dynamic brain scan, F-18 FLT was infused over 1 minute via an infusion pump or by slow bolus, followed by a saline flush. An injected dose of approximately 370 MBq or (10 mCi) maximum was administered. A 70-minute dynamic brain acquisition was then performed. The plasma input function was sampled using either a catheter placed in a radial artery, or using arterialized venous blood using the heated hand methodology (27, 28). Twelve blood samples were rapidly drawn during the first 120 seconds following injection, with additional samples obtained at 3, 4, 5, 7, 10, 15, 20, 30, 45, and 60 minutes post injection. All blood samples were corrected for radiolabeled metabolites by the simplified column chromatography method of Shields (29), and the activity concentration of unmetabolized F-18 FLT in plasma was calculated as a function of time. The F-18 FLT PET images were reconstructed using 3 iterations ordered-subsets expectation-maximization (OSEM) with 32 subsets, and a 2.79mm post-reconstruction Gaussian smoothing filter was

applied. Static images for SUV calculation were computed by combining dynamic time frames from 60–70 min post-injection. Patlak graphical analysis was applied using the metabolite-corrected plasma input function to obtain voxel-wise estimates of the FLT metabolic influx parameter  $K_{i_{max}}$ , also commonly referred to as  $K_{FLT}$  or FLT  $K_{FLUX}$  (15,18–20)).

## Image Analysis

**F-18 FDG PET Imaging**—F-18 FDG PET images were fused with the most recent prior Gd-MRI T1 post contrast images for target lesion confirmation. Visual (qualitative) assessment of F-18 FDG PET and F-18 FLT PET was performed and the de-identified scans were independently scored in random order by two experienced PET readers (JH, KM), based on a 5-point Receiver Operating Curve (ROC) scale as to confidence of tumor recurrence: 1 = definitely recurrence, 2 = probably recurrence, 3 = unable to differentiate recurrence from necrosis, 4 = probably necrosis, 5 = definitely necrosis. The presence of tumor was defined as a value of 1, 2 or 3, and radiation necrosis was defined as a value of 4 or 5. Though the value of 3 indicated an indeterminate lesion, these cases were scored as positive for tumor in the dichotomous paradigm. This designation was made based on similar situations which arise in the clinical setting, where an indeterminate lesion is treated as tumor if not clearly identifiable as necrosis.

For F-18 FDG PET, the maximum standardized uptake value ( $SUV_{max}$ ) with correction for body weight was measured at suspicious area of enhancement on Gd-MRI.  $SUV_{mean}$  and  $SUV_{peak}$  were not recorded because many of the lesions were small and irregular in shape, making such measures subjective and sensitive to user variability in region-of-interest definition and partial volume effect errors. The ratio of F-18 FDG  $SUV_{max}$  of the suspicious lesion to that of the  $SUV_{mean}$  of a 1 cm diameter region of normal (based on F-18 FDG PET and Gd-MRI) contralateral white matter was measured.

**F-18 FLT PET Imaging**—Visual confidence scoring based on a 5-point ROC scale was performed in the same fashion as for F-18 FDG PET scans. Similarly, the FLT  $SUV_{max}$  and  $K_{i_{max}}$  were recorded at the site of the suspicious target lesion on Gd-MRI.

## Data Analysis

Based on 2–33 months of observation, and established by review of the clinical reports with independent agreement by an additional neuroradiologist (LZ), confirmation of recurrent tumor was defined as a definitive increase in size of the lesion by Gd-MRI. Radiation necrosis was defined as stability or regression of this specific lesion over time, even in the face of advancing disease in non-contiguous sites. ROC analysis was performed for both quantitative and visually scored data. Approximate sensitivities and specificities were derived from optimized cut-off values. Differences between recurrent tumor and radiation necrosis for the means of individual quantitative parameters was assessed by the Kruskal-Wallis one-way analysis of variance, with a significance defined as  $p < 0.05$ .

## RESULTS

No adverse events were noted with the use of the investigational imaging agent F-18 FLT. The tumor features, tabulated imaging data, and lesion-specific outcome for each subject are shown in Table 1. Table 2 summarizes the ROC analysis of the continuous (quantitative data). Table 3 summarizes the ROC analysis for the visual confidence scores of the F-18 FDG PET, and F-18 FLT PET scans. Figures 1–3 provide illustrative examples of individual cases. Among the 15 patients enrolled, 10 had glioblastoma multiforme, 3 had grade II oligodendroglioma, one had grade II astrocytoma, and one had oligoastrocytoma. Based on

longitudinal observation by Gd-MRI at the specific site of interest, 11/15 patients proved to have lesion-specific recurrent tumor, while 4/15 had radiation necrosis. Those with radiation necrosis included 3 subjects with glioblastoma multiforme and one with grade II astrocytoma.

Based on the Kruskal-Wallis one-way analysis of variance for non-parametric data, there was a statistically significant difference ( $p = 0.019$ ) between the F-18 FDG  $SUV_{max}$  for tumor (mean 8.19, range 5.3 – 12.1) compared to that for radiation necrosis (mean 5.45, range 4.3 – 6.5). There was also a significant difference ( $p = 0.006$ ) between the F-18 FDG ratio lesion:contralateral white matter (mean 2.83, range 1.83 – 3.96) compared to that for radiation necrosis (mean 1.47, range 1.13 – 2.03). There was a significant difference ( $p = 0.026$ ) between the F-18 FLT  $Ki_{max}$  for tumor (mean 0.0225, range 0.0127 – 0.0294) compared to that for radiation necrosis (mean 0.0109, range 0.0027 – 0.1233). However, there was no significant difference ( $p = 0.068$ ) between the F-18 FLT  $SUV_{max}$  (mean 1.54, range 1.13 – 2.02) for tumor compared to that for radiation necrosis (mean 0.881, range 0.226 – 1.44).

As summarized in Table 2, ROC analysis was performed for the continuous-variable quantitative data (F-18 FDG  $SUV_{max}$ , F-18 FDG ratio lesion:contralateral white matter, F-18 FLT  $SUV_{max}$ , and F-18 FLT  $Ki_{max}$ ). The relative ranking of test performance [area under the curve (AUC), confidence interval (CI)] was as follows: FDG ratio lesion:contralateral white matter > (AUC 0.98, CI 0.91 – 1.00) > F-18 FDG  $SUV_{max}$  (AUC 0.91, CI 0.75 – 1.00) > F-18 FLT  $Ki_{max}$  (AUC 0.89, CI 0.69 – 1.00) > F-18 FLT  $SUV_{max}$  (AUC 0.82, CI 0.56 – 1.00). Within these test (“training”) groups, individual data points were examined and putative optimized cut-off values for quantitative parameters were identified that resulted in the best sensitivities and specificities. For F-18 FDG PET, recurrent tumor was best identified with an ratio of F-18 FDG lesion:contralateral white matter 1.83 (sensitivity 100%, specificity 75%), and an FDG  $SUV_{max}$  6.20 (sensitivity 90.9%, specificity 75%). For F18 -FLT PET, recurrent tumor was best identified by an F-18 FLT  $Ki_{max}$  0.0165 (sensitivity 91%, specificity 75%), and an F-18 FLT  $SUV_{max}$  1.34 (sensitivity 73%, specificity 75%).

As summarized in Table 3, ROC analysis was also performed for visually scored data for F-18 FDG PET and F-18 FLT PET by two experienced nuclear medicine physicians. The ROC AUC for F-18 FDG PET was 0.93 (CI 0.80–1.00). The ROC AUC for F-18 FLT PET was 0.86 (CI 0.67 – 1.00). Based on a predetermined cut-off value of tumor 3 for the visual confidence score, the sensitivity and specificity values were as follows: F-18 FDG PET (sensitivity 91%, specificity 50%); and F-18 FLT PET (sensitivity 81%, specificity 50%).

## DISCUSSION

F-18 FDG PET has been utilized to differentiate recurrent tumor from radiation necrosis in patients with primary brain tumors for nearly 30 years with a broad range of reported sensitivities and specificities (6–11). Recurrent tumor is typically identified by visually-appreciable increased metabolic activity in the lesion of interest, compared to normal white matter. No specific quantitative parameters have been broadly adopted in the distinction of recurrent tumor from radiation necrosis.

Alternative imaging methods have also been employed to distinguish recurrent tumor from radiation necrosis, including magnetic resonance spectroscopy (MRS), which is limited by lack of reimbursement and technical challenges (30,31). Newer MRI techniques, such as arterial spin labeled, and dynamic susceptibility and contrast methods show promise but

require validation (32–34). C-11 methionine and N-13 ammonia PET also show potential (35–39).

A number of studies have suggested that dynamic kinetic modeling is necessary to insure that F-18 FLT uptake is due to specific mechanisms (15, 18–20). Dynamic kinetic modeling requires extended dynamic imaging in a single bed position, limiting analysis to a specific target field-of-view. It is also necessary to draw multiple blood samples, ideally arterial or arterialized venous alternatives, and to process these samples by column chromatography to apply a correction to the input function to account for the contribution of authentic F-18 FLT, versus labeled metabolites. Even if dynamic kinetic modeling of F-18 FLT PET is proven to be of irrefutable value, these methods are unlikely to be broadly adopted in by clinical practice because of the complexity of the procedure. To assess the necessity for dynamic F-18 FLT imaging, we compared both F-18 FLT  $SUV_{max}$  derived from the interval from 60–70 minutes post injection to the metabolite corrected Patlak  $Ki_{max}$ , derived from the plasma input function. There was a significant difference between recurrent tumor and radiation necrosis for F-18 FLT  $Ki_{max}$ , but not for F-18 FLT  $SUV_{max}$ . Although a larger sample size may show a significant difference between recurrent glioma and radiation necrosis for F-18 FLT  $SUV_{max}$ , these data support numerous previous reports that dynamic kinetic modeling of F-18 FLT PET is necessary to ensure optimal results (19,20, 24).

For F-18 FDG  $SUV_{max}$ , F-18 FDG ratio lesion:contralateral white matter and F-18 FLT  $Ki_{max}$ , there was a significant difference between mean values for recurrent tumor and radiation necrosis. The overall ranking of the performance of all quantitative and semi-quantitative tests in distinguishing recurrent tumor from radiation necrosis was as follows: F-18 FDG ratio lesion:contralateral white matter > F-18 FDG  $SUV_{max}$  > F-18 FLT  $Ki_{max}$  > F-18 FLT  $SUV_{max}$ . Each of these parameters showed an equal specificity (75%). Although this would require independent confirmation in a separately validated study, an optimized cut-off lesion:contralateral white matter F-18 FDG ratio of 1.83 for recurrent tumor in this series resulted in the highest sensitivity (100%) in distinguishing recurrent glioma from radiation necrosis.

The visual assessment of the likelihood of tumor by 2 experienced readers also performed well in distinguishing recurrent tumor from radiation necrosis. However, 18% of subjects (2/11) with recurrent tumor and a confidence score of 1 or 2 by F-18 FDG PET had little or no uptake of F-18 FLT in the region of tumor (score of 4 or 5). 50% of patients with radiation necrosis (2/4) had mild F-18 FLT accumulation at the site of radiation necrosis (scored as 3 on the ROC visual confidence score), presumably due to nonspecific leakage of F-18 FLT across a disrupted blood brain barrier. Visual assessment would be expected to vary as a function of reader experience. In clinical practice, where a broad range of reader expertise would be expected, semi-quantitative assessment of F-18 FDG uptake would likely be more reproducible than visual assessment.

## CONCLUSIONS

Although both visual and quantitative assessments of F-18 FDG and FLT uptake on PET performed well, this study suggests that F-18 FLT PET offers no advantage over F-18 FDG PET in the distinction between recurrent tumor and radiation necrosis for moderate and high grade gliomas (grade II). In this series, a ratio of 1.83 of F-18 FDG  $SUV_{max}$  in the target lesion to F-18 FDG  $SUV_{mean}$  in contralateral white matter was the best performing indicator of recurrent glioma (sensitivity 100%, specificity 75%) but requires independent validation.

## Acknowledgments

Conflict of interest and source of funding: This project was funded by the Huntsman Cancer Institute through its Molecular Imaging Research Program, and by grant R01CA135556 (author DK) from the National Cancer Institute (NCI/NIH). The project was also facilitated by a Cancer Center Support Grant from the NCI/NIH (3P30CA042014) and by the Huntsman Cancer Foundation.

## REFERENCES

- Burton EC, Prados MD. Malignant gliomas. *Curr Treat Options Oncol*. 2000; 1:459–468. [PubMed: 12057153]
- Brock CS, Bower M. Current perspectives in gliomas. *Med Oncol*. 1997; 14:103–120. [PubMed: 9330270]
- Collins VP. Gliomas. *Cancer Surv*. 1998; 32:37–51. [PubMed: 10489622]
- Stewart LA. Chemotherapy in adult high-grade glioma: a systematic review and meta-analysis of individual patient data from 12 randomised trials. *Lancet*. 2002; 359:1011–1018. [PubMed: 11937180]
- Stupp R, Mason WP, van den Bent MJ, et al. European Organisation for Research and Treatment of Cancer Brain Tumor and Radiotherapy Groups; National Cancer Institute of Canada Clinical Trials Group. Radiotherapy plus concomitant and adjuvant temozolomide for glioblastoma. *N Engl J Med*. 2005; 10:987–996. [PubMed: 15758009]
- Patronas NJ, Di Chiro G, Brooks RA, et al. Work in progress: [<sup>18</sup>F] fluorodeoxyglucose and positron emission tomography in the evaluation of radiation necrosis of the brain. *Radiology*. 1982 Sep; 144(4):885–889. [PubMed: 6981123]
- Asensio C, Perez-Castejon MJ, Maldonado A, et al. The role of PET-FDG in questionable diagnosis of relapse in the presence of radionecrosis of brain tumors. *Rev Neurol*. 1998; 27:447–452. [PubMed: 9774817]
- Langleben DD, Segall GM. PET in differentiation of recurrent brain tumor from radiation injury. *J Nucl Med*. 2000; 41:1861–1867. [PubMed: 11079496]
- Maldonado A, Santos M, Rodriguez S, et al. The role of PET-FDG in resolving diagnostic doubt: recurrence vs. radionecrosis in brain tumors (abs 124). *Mol Imag Biol*. 2002; 4:S32.
- Thompson TP, Lunsford LD, Kondziolka D. Distinguishing recurrent tumor and radiation necrosis with positron emission tomography versus stereotactic biopsy. *Stereotact Funct Neurosurg*. 1999; 73(1–4):9–14. [PubMed: 10853090]
- Ricci PE, Karis JP, Heiserman JE, et al. Differentiating recurrent tumor from radiation necrosis: time for re-evaluation of positron emission tomography? *AJNR*. 1998; 19:407–413. [PubMed: 9541290]
- Vesselle H, Grierson J, Muzi M, et al. In vivo validation of 3'-deoxy-3'-[<sup>18</sup>F]fluorothymidine ([<sup>18</sup>F]FLT) as a proliferation imaging tracer in humans: correlation of [<sup>18</sup>F]FLT uptake by positron emission tomography with Ki-67 immunohistochemistry and flow cytometry in human lung tumors. *Clin Cancer Res*. 2002; 8:3315–3323. [PubMed: 12429617]
- Vesselle H, Grierson J, Peterson LM, et al. [<sup>18</sup>F]-Fluorothymidine radiation dosimetry in human PET imaging studies. *J Nucl Med*. 2003; 44:1482–1488. [PubMed: 12960196]
- Rasey JS, Grierson JR, Wiens LW, et al. Validation of FLT uptake as a measure of thymidine kinase-1 activity in A549 carcinoma cells. *J Nucl Med*. 2002; 43:1210–1217. [PubMed: 12215561]
- Brockenbrough JS, Souquet T, Morihara JK, et al. Tumor 3'-Deoxy-3'-18F-Fluorothymidine (18F-FLT) Uptake by PET Correlates with Thymidine Kinase 1 Expression: Static and Kinetic Analysis of 18F-FLT PET Studies in Lung Tumors. *J Nucl Med*. 2011; 52:1181–1188. [PubMed: 21764789]
- Schwartz JL, Tamura Y, Jordan R, et al. Monitoring tumor cell proliferation by targeting DNA synthetic processes with thymidine and thymidine analogs. *J Nucl Med*. 2003; 44:2027–2032. [PubMed: 14660729]
- Shields AF, Grierson JR, Dohmen BM, et al. Imaging proliferation in vivo with [<sup>18</sup>F]FLT and positron emission tomography. *Nat Med*. 1998; 4:1334–1336. [PubMed: 9809561]

18. Shields AF, Briston DA, Chandupatla S, et al. Evaluation of analytical methods. *Eur J Nucl Med Mol Imaging*. 2005; 32(11):1269–1275. [PubMed: 15991018]
19. Muzi M, Mankoff DA, Grierson JR, et al. Kinetic modeling of 3'-deoxy-3'-fluorothymidine in somatic tumors: mathematical studies. *J Nucl Med*. 2005; 46:371–380. [PubMed: 15695799]
20. Muzi M, Vesselle H, Grierson JR, et al. Kinetic analysis of 3'-deoxy-3'-fluorothymidine PET studies: validation studies in patients with lung cancer. *J Nucl Med*. 2005; 46:274–282. [PubMed: 15695787]
21. Choi SJ, Kim JS, Kim JH, et al. [18F]3-deoxy-3-fluorothymidine PET for the diagnosis and grading of brain tumors. *Eur J Nucl Med Mol Imaging*. 2005; 32:653–659. [PubMed: 15711980]
22. Chen W, Cloughesy T, Nirav Kamdar N, et al. Imaging Proliferation in Brain Tumors with <sup>18</sup>F-FLT PET: Comparison with F-18 FDG. *J Nucl Med*. 2005; 46:945–952. [PubMed: 15937304]
23. Jacobs AH, Thomas A, Kracht LW, et al. 18F-fluoro-L-thymidine and 11C-methylmethionine as markers of increased transport and proliferation in brain tumors. *J Nucl Med*. 2005; 46:1948–1958. [PubMed: 16330557]
24. Spence AM, Muzi M, Link JM, et al. NCI-sponsored trial for the evaluation of safety and preliminary efficacy of 3'-deoxy-3'-[18F]fluorothymidine (FLT) as a marker of proliferation in patients with recurrent gliomas: preliminary efficacy studies. *Mol Imaging Biol*. 2009; 11:343–355. [PubMed: 19326172]
25. Spence AM, Muzi M, Link JM, et al. NCI-sponsored trial for the evaluation of safety and preliminary efficacy of FLT as a marker of proliferation in patients with recurrent gliomas: safety studies. *Mol Imaging Biol*. 2008; 10(5):271–280. [PubMed: 18543042]
26. Reischl G, Blocher A, Wei R, et al. Simplified, automated synthesis of 3'-(18F)fluoro-3'-deoxythymidine ((18F)FLT) and simple methods for metabolite analysis in plasma. *Radiochim Acta*. 2006; 94:447–351.
27. Sonnenberg GE, Keller U. Sampling of arterialized heated-hand venous blood as a noninvasive technique for the study of ketone body kinetics in man. *Metabolism*. 1982; 31:1–5. [PubMed: 6804743]
28. Copeland KC, Kenney FA, Nair KS. Heated dorsal hand vein sampling for metabolic studies: a reappraisal. *Am J Physiol*. 1992; 263(5 Pt 1):E1010–E1014. [PubMed: 1443110]
29. Shields AF, Briston DA, Chandupatla S, et al. A simplified analysis of [18F]3'-deoxy-3'-fluorothymidine metabolism and retention. *Eur J Nucl Med Mol Imaging*. 2005; 32:1269–1275. [PubMed: 15991018]
30. Rock JP, Hearshen D, Scarpace L, et al. Correlations between magnetic resonance spectroscopy and image-guided histopathology, with special attention to radiation necrosis. *Neurosurgery*. 2002; 51:912–919. discussion 919–920. [PubMed: 12234397]
31. Dowling C, Bollen AW, Noworolski SM, et al. Preoperative proton MR spectroscopic imaging of brain tumors: correlation with histopathologic analysis of resection specimens. *AJNR*. 22:604–612.
32. Ozsunar Y, Mullins ME, Kwong K, et al. Glioma recurrence versus radiation necrosis? A pilot comparison of arterial spin-labeled, dynamic susceptibility contrast enhanced MRI, and FDG-PET imaging. *Acad Radiol*. 2010; 17:282–290. [PubMed: 20060750]
33. Narang J, Jain R, Arbab AS, Mikkelsen T, et al. Differentiating treatment-induced necrosis from recurrent/progressive brain tumor using nonmodel-based semiquantitative indices derived from dynamic contrast-enhanced T1-weighted MR perfusion. *Neuro Oncol*. 2011 Sep; 13(9):1037–1046. [PubMed: 21803763]
34. Fatterpekar GM, Galheigo D, Narayana A, et al. Treatment-related change versus tumor recurrence in high-grade gliomas: a diagnostic conundrum—use of dynamic susceptibility contrast-enhanced (DSC) perfusion MRI. *AJR Am J Roentgenol*. 2012 Jan; 198(1):19–26. Review. [PubMed: 22194475]
35. Tripathi M, Sharma R, Varshney R, et al. Comparison of F-18 FDG and C-11 methionine PET/CT for the evaluation of recurrent primary brain tumors. *Clin Nucl Med*. 2012 Feb; 37(2):158–163. [PubMed: 22228339]
36. D'Souza MM, Jaimini A, Tripathi M, et al. F-18 FDG and C-11 methionine PET/CT in intracranial dural metastases. *Clin Nucl Med*. 2012 Feb; 37(2):206–209. [PubMed: 22228356]

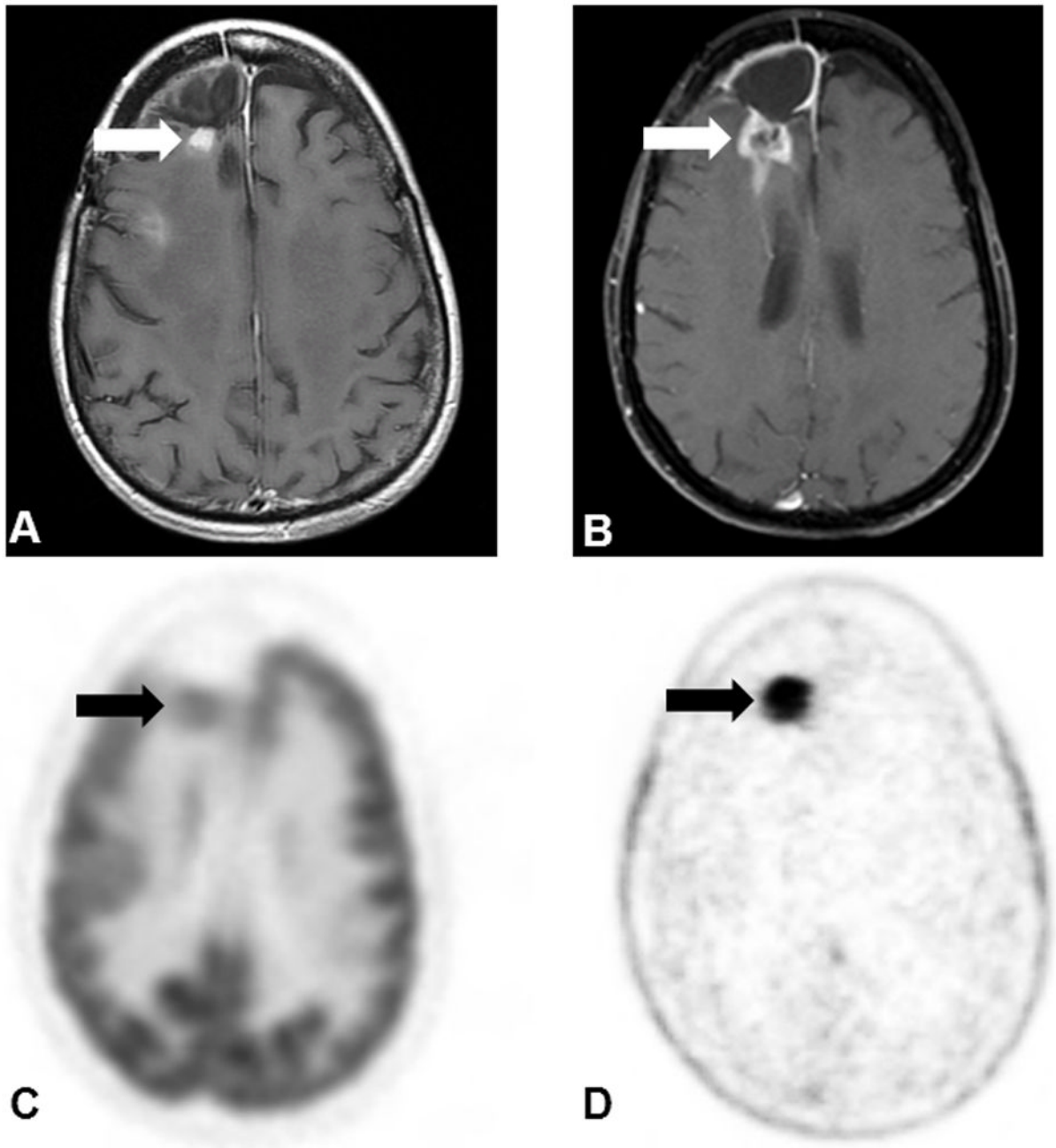


37. Terakawa Y, Tsuyuguchi N, Iwai Y, et al. Diagnostic accuracy of 11C-methionine PET for differentiation of recurrent brain tumors from radiation necrosis after radiotherapy. *J Nucl Med.* 2008; 49:694–699. [PubMed: 18413375]
38. Chung JK, Kim YK, Kim SK, et al. Usefulness of 11C-methionine PET in the evaluation of brain lesions that are hypo- or isometabolic on FDG PET. *Eur J Nucl Med Mol Imaging.* 2002; 29:176–182. [PubMed: 11926379]
39. Xiangsong Z, Weian C. Differentiation of recurrent astrocytoma from radiation necrosis: a pilot study with 13N-NH3 PET. *J Neurooncol.* 2007; 82:305–311. [PubMed: 17120157]

\$watermark-text

\$watermark-text

\$watermark-text

**FIGURE 1.**

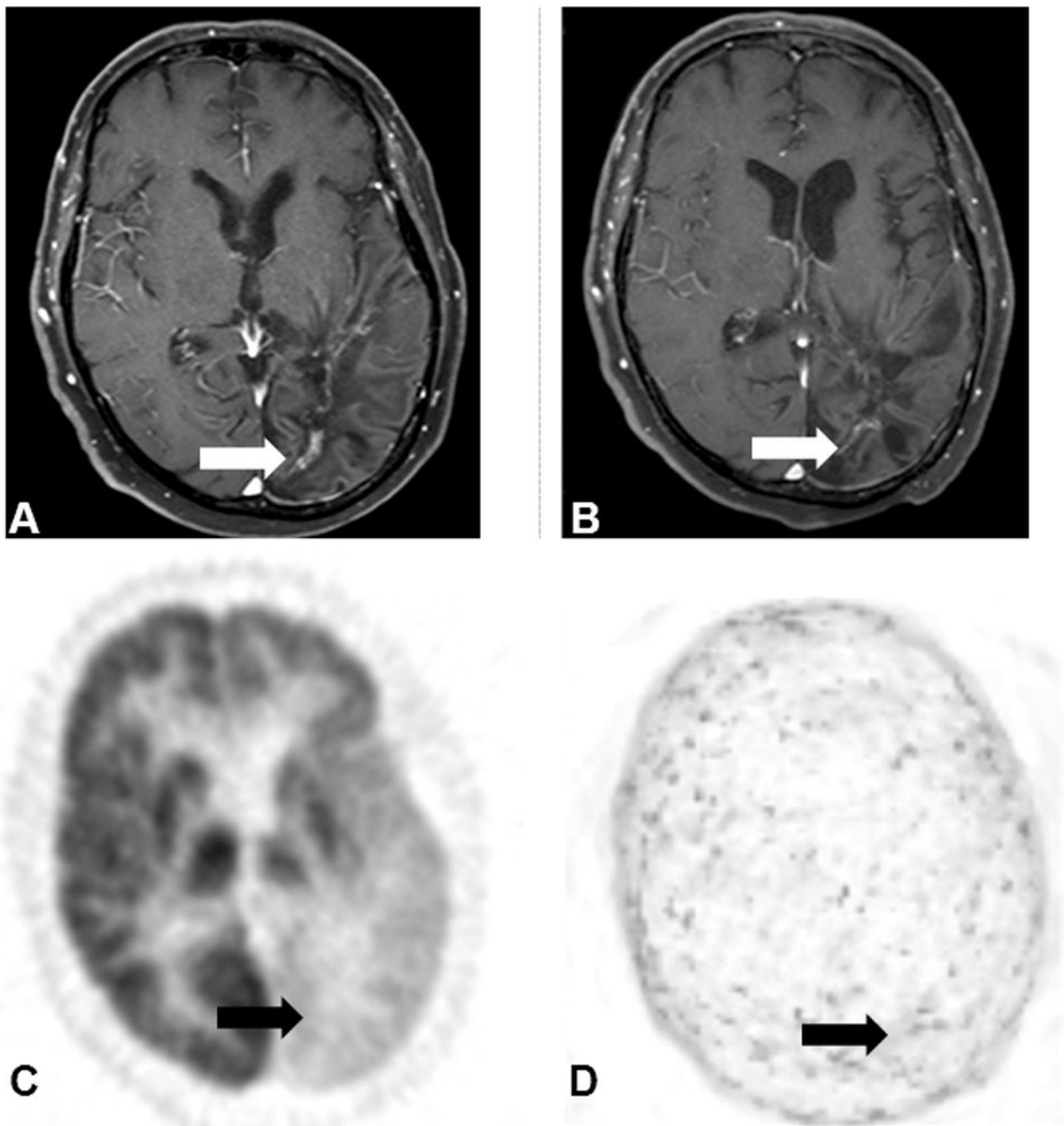
True positive study for recurrent tumor. 47 year old female (subject 8) with initial multifocal glioblastoma multiforme was treated with surgical debulking, radiation and chemotherapy with initial good response. Follow-up Gd-MRI (A) showed new focus of enhancement in the posterior right frontal lobe, along the margin of a resection cavity and within the radiation field consistent with either recurrent tumor or radiation necrosis. F-18 FDG PET scan (C) performed after MRI (A) showed increased uptake consistent with recurrent tumor (SUVmax 7.9, F-18 FDG ratio lesion:contralateral white matter 2.63). F-18 FLT PET (D) scan also confirmed intense uptake (SUVmax 1.764, Kimax 0.0253), also consistent with

recurrent tumor. Follow-up Gd-MRI (B) showed clear progression of enhancing mass consistent with recurrent tumor.

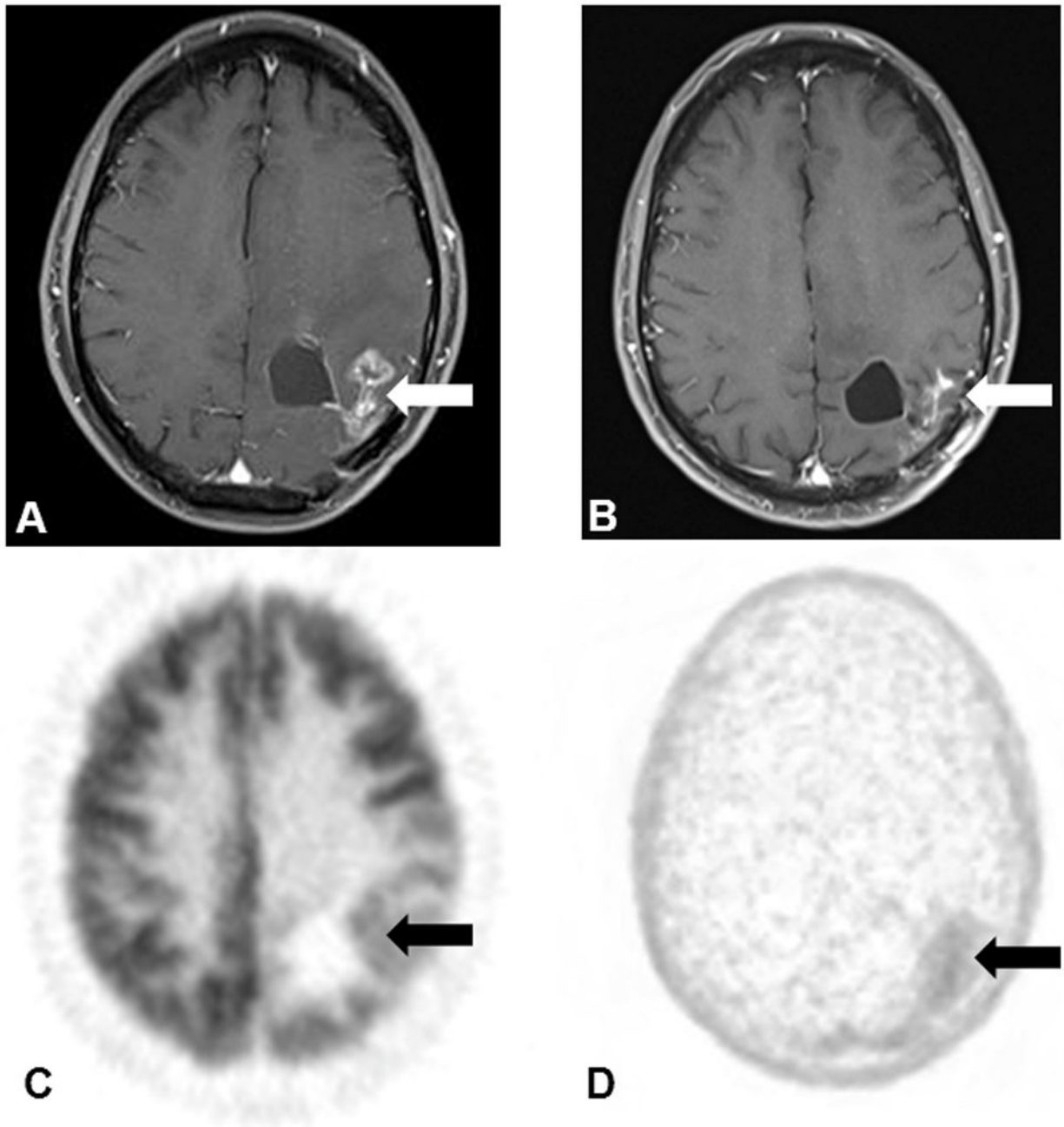
\$watermark-text

\$watermark-text

\$watermark-text

**FIGURE 2.**

True negative study for recurrent tumor. 61 year old male (subject 4) with a left occipital glioblastoma multiforme was treated with radiation and chemotherapy with initial good response. Follow-up Gd-MRI (A) showed new focus of enhancement within the radiation bed in the left occipital lobe. F-18 FDG PET scan (C) performed after MRI (A) showed no increased uptake above that of white matter (SUVmax 5.2, F-18 FDG ratio lesion:contralateral white matter 1.182). F-18 FLT PET (D) scan also confirmed no appreciable uptake (SUVmax 1.29, Kimax 0.0128), confirming impression of radiation necrosis. Follow-up MRI (B) and subsequent MRI scans showed sustained regression of the region of enhancement, consistent with radiation necrosis.

**FIGURE 3.**

False positive study for recurrent tumor. 39 year old male (subject 11) with grade II left parietal grade II astrocytoma was treated with surgical debulking, radiation and chemotherapy with initial good response. Follow-up MRI (A) showed new focus of enhancement in the left parietal lobe, along the margin of a resection cavity. F-18 FDG PET scan (C) performed after Gd-MRI (A) showed appreciable but mild uptake greater than that of contralateral white matter (SUVmax 6.5, F-18 FDG ratio lesion:contralateral white matter 2.031). F-18 FLT PET (D) scan also demonstrated mild uptake in the tumor bed (SUVmax 1.44, Kimax 0.0233). Follow-up Gd-MRI (B) and subsequent Gd-MRI's showed clear and sustained regression of enhancing lesion, consistent with radiation necrosis.

\$watermark-text

\$watermark-text

\$watermark-text

Table 1

Data by Subject

	Tumor Type	Lesion Outcome	FDG SUVmax	FDG ratio lesion:white matter	FLT SUVmax	FLT Kimax	FDG visual confidence	FLT visual confidence
1	Oligodendroglioma Grade II	Recurrent Tumor	8.92	3.304	1.785	0.0247	2	2
2	Glioblastoma Multiforme	Recurrent Tumor	8.13	3.127	1.774	0.0241	2	2
3	Glioblastoma Multiforme	Recurrent Tumor	6.3	2.25	1.859	0.0294	1	2
4	Glioblastoma Multiforme	Radiation Necrosis	5.2	1.182	1.29	0.0128	4	5
5	Oligodendroglioma Grade II	Recurrent Tumor	6.6	2.129	1.174	0.0219	1	2
6	Oligoastrocytoma Grade II	Recurrent Tumor	12.1	3.27	1.164	0.0127	1	4
7	Glioblastoma Multiforme	Radiation Necrosis	4.3	1.129	0.226	0.0027	4	3
8	Glioblastoma Multiforme	Recurrent Tumor	7.9	2.633	1.764	0.0253	1	1
9	Glioblastoma Multiforme	Recurrent Tumor	7.4	2.552	2.022	0.0236	4	1
10	Oligodendroglioma Grade II	Recurrent Tumor	6.2	2.385	1.411	0.0255	1	2
11	Astrocytoma Grade II	Radiation Necrosis	6.5	2.031	1.44	0.0233	3	3
12	Glioblastoma Multiforme	Radiation Necrosis	5.8	1.526	0.566	0.0047	3	4
13	Glioblastoma Multiforme	Recurrent Tumor	5.3	1.828	1.552	0.0165	1	5
14	Glioblastoma Multiforme	Recurrent Tumor	10.2	3.643	1.127	0.0255	1	1
15	Glioblastoma Multiforme	Recurrent Tumor	11.1	3.964	1.34	0.0181	1	2

\* Visual scoring was based on a 5-point ROC scale as to confidence of tumor recurrence: 1=definitely recurrence, 2 probably recurrence, 3= unable to differentiate recurrence from necrosis (mathematically assumed to be tumor), 4= probably necrosis, 5= definitely necrosis.

**Table 2**

Summary ROC Analysis for Quantitative Continuous Data

<b>Statistical parameter</b>	<b>FDG SUVmax</b>	<b>FDG ratio lesion:white matter</b>	<b>FLT SUVmax</b>	<b>FLT Ki-max</b>
Area under ROC* curve	0.93	0.98	0.86	0.89
95% CI	0.75 – 1.00	0.91 – 1.00	0.56 – 1.00	0.69 – 1.00
Optimized cut-off, tumor if:	6.20	1.83	1.34	0.0165

**Table 3**

Summary of ROC Analysis of Visually Scored Data\*

Parameter	Estimated Value	FDG PET 95% Confidence Interval		Number Correct: 12/15 Recurrent tumor cases missed: 1 Radiation necrosis cases missed: 2 ROC AUC: 0.932
		Lower Limit	Upper Limit	
Sensitivity	90.9%	0.571	0.995	
Specificity	50.0%	0.092	0.908	
PPV	80.0%	0.514	0.947	
NPV	20.0%	0.053	0.486	

Parameter	Estimated Value	FDG PET 95% Confidence Interval		Number Correct: 12/15 Recurrent tumor cases missed: 0 Radiation necrosis cases missed: 3 ROC AUC: 0.864
		Lower Limit	Upper Limit	
Sensitivity	82.1%	0.679	1.000	
Specificity	50.0%	0.013	0.781	
PPV	73.3%	0.660	0.997	
NPV	26.7%	0.003	0.340	